

The Manufacture and Test of (110) Orientated Silicon Based Micro Heat Exchanger

Shung-Wen Kang, Yu-Tang Chen and Guang-Shang Chang

*Department of Mechanical and Electro-Mechanical Engineering
Tamkang University
Tamsui, Taiwan 251, R.O.C.
E-mail: david1@mail.tku.edu.tw*

Abstract

The micro cross-flow heat exchanger made of (110)-orientated silicon is fabricated by bulk micromachining that is compatible with semiconductor producing processes, and wafers with hundreds of high aspect ratio channels are bonded together by diffusion bonding with aluminum as medium layers.

The core of the micro heat exchanger is about 0.918 cm^3 , and the density of the heat transfer area is $15,294 \text{ m}^2/\text{m}^3$. Using pure water as the working fluid, the Reynolds Numbers show that the fluid field is always laminar flow, and as the maximum pressure drop reaches 2.47 bar, the flow rate is greater than 4.5 L/min. The heat transfer measured between hot and cold fluid is 5 kW; the log mean temperature is greater than 30 K, and that makes the overall heat transfer coefficient up to $24.7 \text{ kW/m}^2\text{-K}$, corresponds to a volumetric heat transfer coefficient of $188.5 \text{ MW/m}^3\text{-K}$.

Except reacted on a few special chemicals, silicon has excellent properties in mechanics, heat transfer, and anti-corrosion, so the (110) silicon based micro heat exchanger suits for the operations at high temperature or in corrosive fluids.

The extremely small heat sink appears to have a variety of current and potential applications in areas such as micro-electronic cooling and biomedical processes where high heat transfer power are required with little weight and small volume.

Key Words: Micro Cross-Flow Heat Exchanger, Bulk Micromachining, Heat Transfer Area, Pressure Drop, Heat Transfer Coefficient

1. Introduction

The development of micro heat exchanger began with solving the problem of heat dissipation in VLSI. In 1984, Tuckerman [1] used anisotropic etching and precision mechanical sawing techniques to manufacture about $280 \text{ }\mu\text{m}$ deep microchannels in $500 \text{ }\mu\text{m}$ thick (110) orientated silicon wafers. He reported a hybrid of direct contact and cold plate technologies using laminar

water flow in the micropassages and absorbing heat flux of 150 W/cm^2 .

Both Cross and Ramshaw [2] reported on a type of heat exchanger called printed circuit heat exchanger. The channels on the plates of the special heat exchanger were machined by using chemical etching methods, and the plates were bonded together by diffusion brazing. The channel size is 0.4 mm wide and 0.3 mm deep, and the volumetric heat transfer coefficient is $7 \text{ MW/m}^3\text{-K}$.

High-capacity micro heat exchangers have also been produced using diamond machining techniques by Friedrich and Kang [3], however, the processes are not easy for batch-fabrication. In the present work, the channel and complete device fabrication is using silicon wet etching techniques. The typical process include mask-making, photoresist coating and baking, exposing, etching and cleaning.

The anisotropic etching of SCS was discovered in the early 1960s. In 1969, Lee [4] etched silicon wafers by organic etchants, and he found that the etching rates on (111) were very slow. Bean [5] reported that the extremely high ratio greater than 650 to 1 were obtained in (110) orientation-dependent etching. Bean reported that the etching rate of (110) silicon in 35% *w.t.* KOH was about 0.8 $\mu\text{m}/\text{min}$. at 80 $^{\circ}\text{C}$; Krause and Obermeyer [6] proved that the etching rate and the aspect ratio of etched channels would increase with the concentration of KOH liquor in recent report. Studies of conventional compact heat exchangers design theories were already completed by Kays and London [7].

The metallic heat exchanger [8] with features that range in size from 150-750 μm have thermal resistances ranging from 0.07 to 0.12 $^{\circ}\text{C}/\text{W cm}$ at flow rates of water of ~ 20 L/h and pressures of $8.6\text{--}83 \times 10^3$ N/m^2 and fabricated using sacrificial polymer mandrils.

N. Saji, et al. [9] developed a compact laminar flow heat exchanger with stainless steel micro-tube, which consists of 12 elements with a total of 4800 stainless steel micro-tube. Each element is formed with 400 tubes that have an inner diameter of 0.5 mm, an outer diameter of 0.7 mm and is 310 mm long.

In the major processes of fabricating the silicon based micro heat exchanger, bonding is the key point. Direct bonding is one of the major bonding methods in semiconductor processes by the hydrate bonding on the wafer and heat treatments in high temperature atmosphere. Except anodic bonding and direct bonding, the diffusion bonding is the well-chosen method to bond silicon wafer together in lower temperature.

Because only a few studies in the micro heat exchangers area have been reported, researches are needed to investigate the basic design, fabrication and performance of the micro heat exchangers to expand the developments and strengthen their reliability. The objectives of this research were

referred to design, fabricate and test a (110) silicon based micro cross-flow heat exchanger.

2. Design

A cross-flow arrangement was adopted in this micro heat exchanger design because this arrangement greatly simplified the header design at the entrance and exit of each fluid. A generic design for a two-fluid, cross-flow plate heat exchanger is shown in Figure 1.

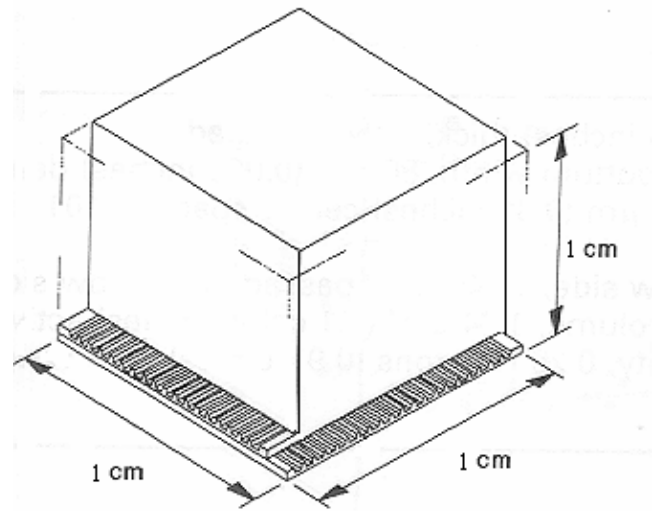


Figure 1. A generic plate-type cross-flow micro heat exchanger

The purpose for using micro channels is to achieve specific heat transfer performance, U , within minimum weight, material and volume constraints. Since the heat transfer in hot and cold fluids are

$$Q_h = m_h c_{h,m} (T_{h,i} - T_{h,o}) \quad (1)$$

$$Q_c = m_c c_{c,m} (T_{c,o} - T_{c,i}) \quad (2)$$

and the average heat transfer is

$$Q_m = 1/2 (Q_h + Q_c) \quad (3)$$

the overall heat transfer coefficient can be calculated from

$$U = \frac{Q_m}{A \cdot \Delta T_m \cdot F} \quad (4)$$

Where A is the total heat transfer area on one side, and F is the correction factor for a cross-flow heat exchanger with both fluids unmixed. The log mean temperature difference

$$\Delta T_m = \frac{(T_{h,i} - T_{c,i}) - (T_{h,o} - T_{c,i})}{\ln\left(\frac{T_{h,i} - T_{c,i}}{T_{h,o} - T_{c,o}}\right)} \quad (5)$$

The total volumetric heat transfer surface coefficient could be expressed as

$$U_v = U \cdot B \quad (6)$$

In which is the heat exchanger heat transfer surface area per unit volume. The overall heat transfer coefficient may be expressed as

$$\frac{1}{UA} = \frac{1}{h_h A} + R_w + \frac{1}{h_c A} \quad (7)$$

Due to the high thermal conductivity of silicon and the small wafer thickness, a simple calculation shows that the thermal resistance of the wall (R_w) could be negligible compared with the convection resistance. Because the channels on the two sides have almost the same geometry, mass flow rate, and heat transfer conditions, it is reasonable to assume that the convection heat transfer coefficient must be the same on both sides, therefore

$$h_h \cong h_c \cong h \quad (8)$$

and simplify it sequentially to

$$h = 2U \quad (9)$$

The Nusselt Number is of the form

$$Nu = \frac{h D_h}{k_f} \quad (10)$$

The great advantage of using thin silicon wafers with micro flow channels is the ability to produce a very large ratio of heat transfer area per unit volume. In addition, the large thermal resistance between the heat exchanger plates is very low due to the thin, high conductivity silicon walls. The cross-flow heat exchanger is made by stacking and bonding silicon wafers together which have had flow channels etched into them by lithography. The factors that need to be addressed in the design of any of these devices include heat transfer capacity, pressure drop, size and number of channels, spacing between channels, and internal deformation due to differential pressure and temperature.

Any consideration of mechanical devices made from silicon must certainly take into account the mechanical behavior and properties of single-crystal-silicon. The Young's modulus of silicon is 1.9×10^7 N/cm², and has a value approaching that of stainless steel. The Knoop

hardness of silicon (850 kg/mm²) is almost twice as high as nickel and iron. SCS has a tensile yield strength of 6.9×10^5 N/cm², which is at least 3 times higher than stainless steel wire.

3. Fabrication

Lithography technology is widely used for semi-conductor processes; it includes wafers-cleaning, growth of etching mask, photoresist coating, exposure and develop, etching, doping, etc., almost all of them made a contribution to this study.

Three etchant systems are of particular interest due to their versatility: ethylene diamine pyrocatechol (EDP) and water, KOH and water, HF, HNO₃, and acetic acid, (CH₃COOH). In this study, KOH system was used. KOH and water is orientation dependent and, in fact, exhibits much higher (110) to (111) etching rate ratio than EDP, and for this reason it is especially useful for grooves etching on (110) wafers since the large differential etching ratio permits deep, high aspect ratio grooves with minimal undercut of the mask. Si₃N₄ is the preferred masking material for high aspect ratio, long KOH etching channels. We used 120 nm silicon nitride and 180 nm silicon dioxide as the etching mask.

The concentration of etchant also influences the etching rate effectively. The etching rate would ascend with the quantity of hydrate in liquor. Generally speaking, the etching rate of 40% w.t. would be larger than that of 25% w.t., because the hydrate in 25% w.t. KOH are more than that in 40% w.t. KOH.

Temperature affects etching rate significantly. The etching rate and temperature have a relation that could be expressed as

$$R = R_0 \exp(-E_c/kT) \quad (11)$$

The R_0 represents the Pre-Exponential Factor; in eq. (11), we understand that the etching rate will raise apparently with temperature. K. E. Bean reported that the (110) wafers were etched at about 0.8 μ m/min. in 50% w.t. KOH at 80 °C. In our study 40% w.t. KOH with stirring at 65 °C was adopted, and it took about 400 minute to etch a 200 μ m deep channel; the misalignment was about 3°~5°, so that the undercut beside the 40 mm wide channel was about 5~10 μ m. Figure 2 shows the micrograph of the channels on the wafer.

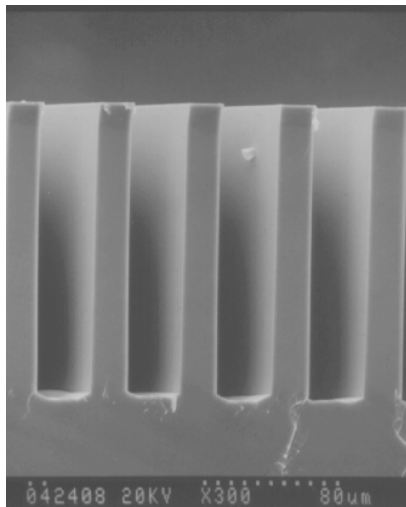


Figure 2. The micrograph of the channels on the wafer (wafer thickness: 370 μm , cross section of the channels: 40 $\mu\text{m} \times 200 \mu\text{m}$, bottom thickness: 170 μm , fin width: 40 μm)

The pattern we designed is 15 mm wide and 25 mm long, and the channel area is 10 mm wide by 10 mm long; there are 125 channels with 40 μm width and 200 μm depth in the channel area.

Temperature is the most influential variable during diffusion bonding. In any thermally activated process an incremental change in temperature will cause the greatest change in process kinetics when compared to most other process variables. In addition, virtually all the mechanisms in diffusion bonding are temperature dependent. In general, the temperature at which diffusion bonding will take place is above one half of the absolute melting temperature.

Time is closely related to temperature in which most diffusion controlled reaction rates vary with time. Experience indicates that increasing both the time and the pressure at bonding temperature increase joint strength up to a limit. Beyond this point no further gains are achieved.

Pressure is important just in the beginning when the bonding takes place. Oxide layers will fracture and the grains will deform and contact one another between the working pieces if necessary pressure is given, but as the diffusion is ongoing, pressure is not as important as in the beginning. In this research low pressure is employed to avoid the thin walls on the silicon wafers being bulked, and the pressure of 240 kg/cm^2 was used for clamping the wafers

Silicon has a high melting point of more than 1400 $^{\circ}\text{C}$, and the temperature at which the diffusion bonding takes place would high enough to increase the complexity, for this reason, a low melting point

medium material will lower the bonding temperature, in addition, aluminum has a good diffusion property with silicon, so we consider aluminum foils as the medium layers in the bonding processes.

In this research, the aluminum foils were cleaned in a 5% hydrochloric acid for 5 minutes with ultrasonic shaking to remove alumina on the foils, and the silicon wafers were cleaned by the same way in lithography. The foils and wafers are then stacked and clamped in a graphite clamp, and they were placed in a diffusion bonding furnace, and were heated to 600 $^{\circ}\text{C}$ for one hour, and the vacuum was approximately 15 μtorr . A micrograph of an edge of the micro heat exchanger is shown in Figure 3. Figure 4 shows the packaged micro heat exchanger by a 10-dollar coin.

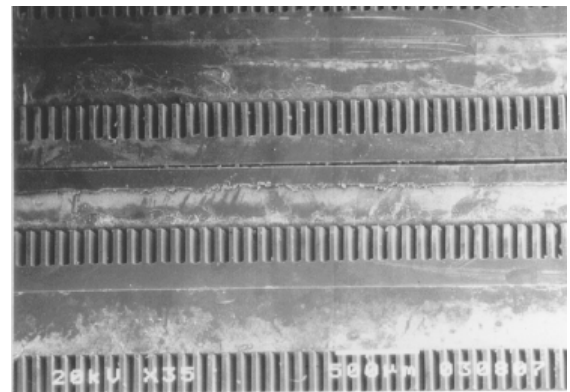


Figure 3. A micrograph of an edge of the micro heat exchanger



Figure 4. The micro heat exchanger (channel heat transfer length: 0.9 cm, number of channel on each wafer: 125, number of wafer layers: 26, number of channels on one side: 1625, free flow area: 13 mm^2 , free flow area/ frontal area: 12.7 %, total heat transfer area on one side: 70.2 cm^2 , total heat transfer volume: 0.918 cm^3 , total heat transfer area/ total volume: 15295 m^2/m^3)

4. Test

Figure 5 shows a schematic of the experimental apparatus used to test the micro heat exchanger. To minimize the amount of equipment required, measurements were made using only DI water as the working fluid on both hot and cold side of the heat exchanger. A test setup contains separate measuring devices for measuring the flow, as well

as pressure and temperature at both inlets and outlets of the micro heat exchanger. The hot and cold water was supplied in a close circuit from hot and cold water tank. The same flow rate was used for both streams by adjusting the control valves. The water pressure and temperature were measured at the inlets and outlets respectively.

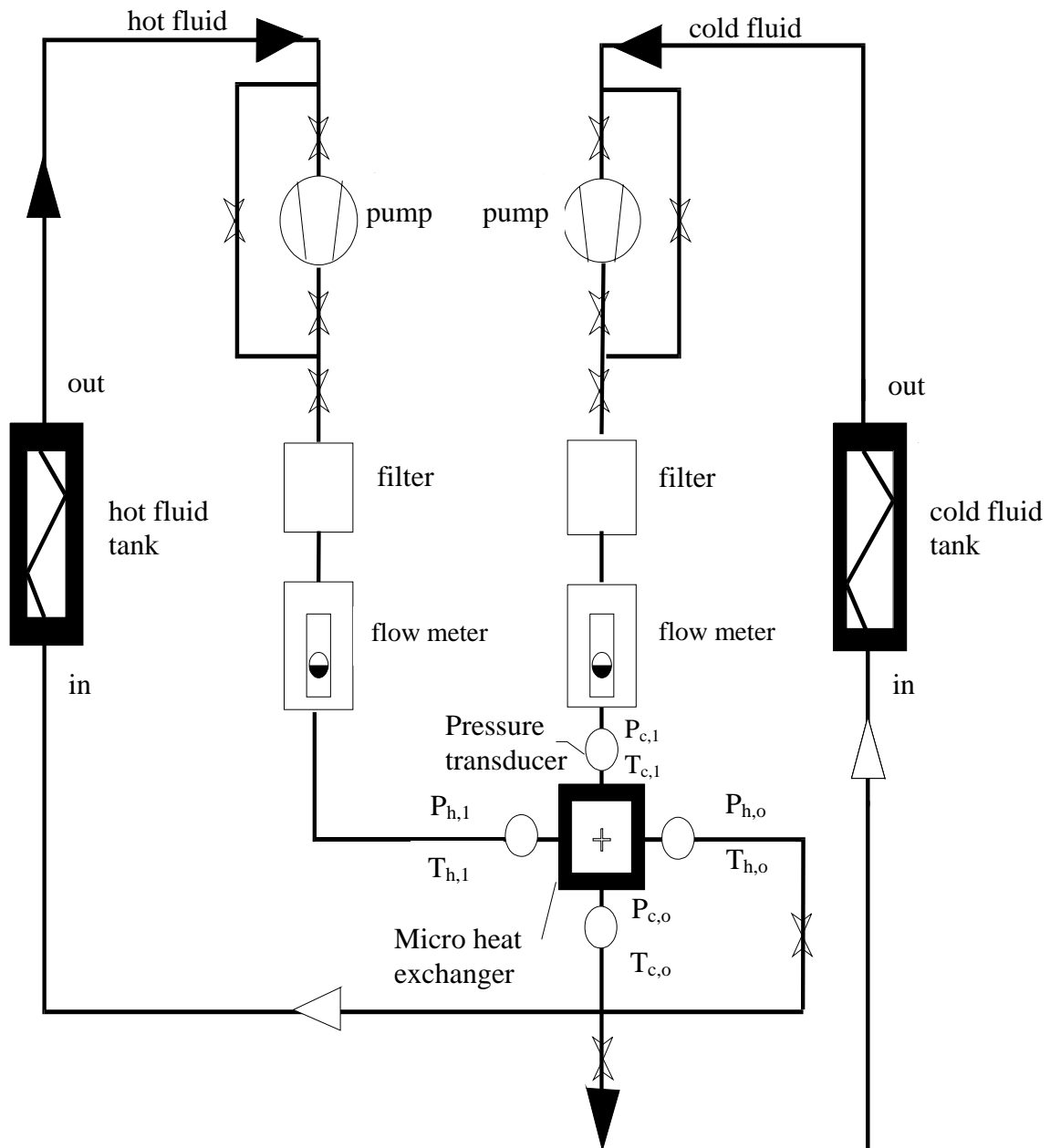


Figure 5. Schematic of the experimental apparatus

The data obtained in the experiments were pressure drop, flow rates, inlet and outlet temperatures from the both sides of the heat exchanger; the flow rates of both sides were kept the same by controlling the valves. The experimental procedures consisted of varying the flow rates and measuring the pressures, temperatures, and the flow

rates.

The calculations were carried out according to equations based on a single-pass, cross-flow heat exchangers with both the hot and cold water unmixed. From the measurements of the mass flow rate, inlet and outlet temperatures, Reynolds number (Re), the heat transfer (Q), the

corresponding overall heat transfer coefficient (h), volumetric heat transfer coefficient (U_v) and could be calculated.

Figure 6 shows the measured pressure drop on the hot side and cold side as a function of the water flow rate. We found the maximum pressure drop reached 2.47 bar when flow rate is 4.5 L/min. As we kept the inlet temperatures both the hot and cold side in the same region, and only adjusted the flow rates, we could obtain corresponding log mean temperature differences, and they are shown in Figure 7.

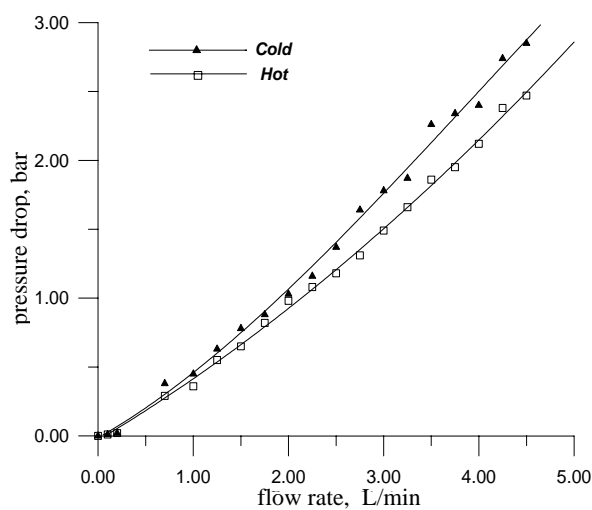


Figure 6. Measured pressure drop as a function of the flow rate

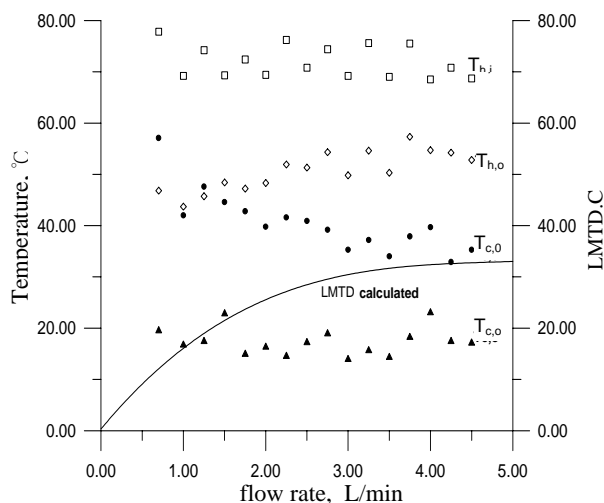


Figure 7. Relationship of the temperature and the flow

In Figure 8 the overall heat transfer coefficient (U) and the volumetric heat transfer coefficient (U_v) calculated from the measured data has been plotted versus the Reynolds number on the both sides. The highest measured U , 24.7 kW/m²-K, corresponds to an U_v of 188.5 MW/m³-K. The Reynolds number

for the maximum flow rate measured were 820 on the hot side, and 440 on the cold side, that is, only laminar flow occurred over the test range. Figure 9 shows the Nusselt number variation with Reynolds number for both the hot and cold sides. The difference between the two curves is that the Reynolds number range on the hot side is greater than that of the cold side due to the variation of the viscosity.

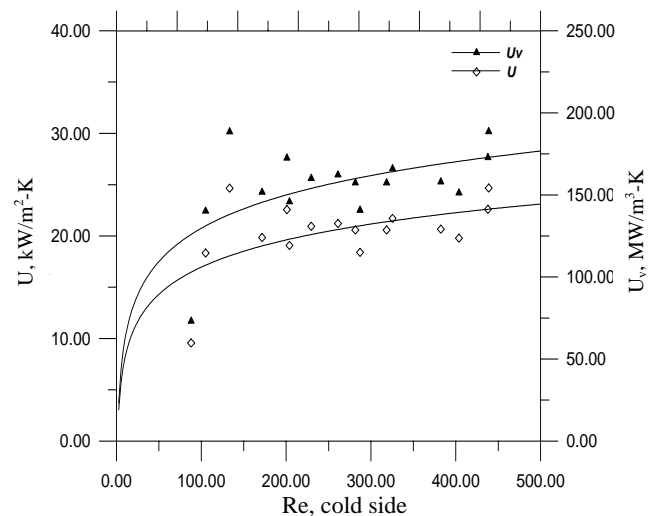


Figure 8(a). U and U_v as a function of Re on both cold sides

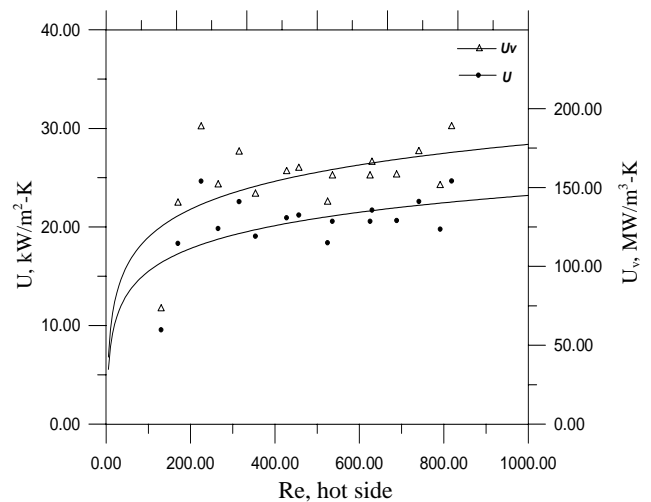


Figure 8(b). U and U_v as a function of Re on hot sides

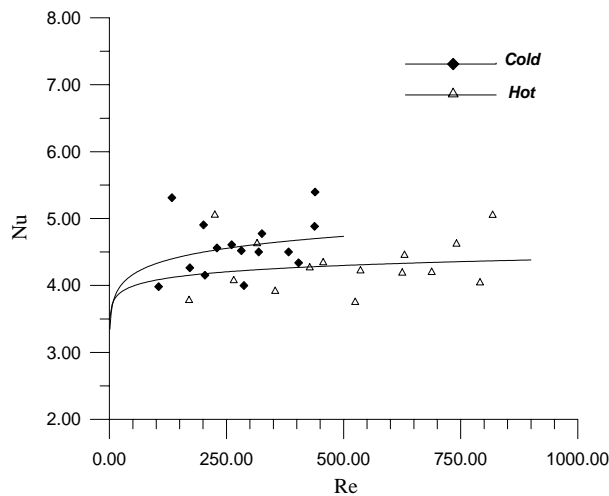


Figure 9. Nu as a function of Re on both hot and cold sides

5. Conclusion

Micro manufacturing techniques such as lithography processes and vacuum diffusion bonding were adopted to fabricate the silicon based micro heat exchangers, which have dimensions an order of magnitude smaller than in conventional compact heat exchanger. Potential applications for the heat exchanger are seen in areas such as microelectronics cooling, aircraft, aerospace cooling and biomedical processes where high heat transfer power are required with little weight and small volume.

A test system was developed to measure micro heat exchanger flow-friction and thermal performance. Using DI water as the working fluid, about 5 kW of energy could be transferred in a cubical heat transfer volume of 0.918 cm³ with a log mean temperature difference of about 30 K. This corresponds to a overall heat transfer coefficient of more than 24.7 kW/m²-K, and volumetric heat transfer coefficient of 188.5 MW/m³-K.

Nomenclature

A	heat exchanger total transfer area on one side
B	ratio of total heat transfer area on one side of the exchanger to total volume of the exchanger
c	specific heat
D _h	hydraulic diameter
E _c	reactive activation energy
F	heat exchanger correction factor
h	heat convection coefficient
k	Boltzmann constant

k _f	thermal conductivity of working fluid
m	mass flow rate
Nu	Nusselt Number
Q	heat transferred
R	reactive rate
R _w	thermal resistance of wall
T	temperature
U	overall heat transfer coefficient
U _v	volumetric heat transfer coefficient

Subscripts

c	cold fluid
h	hot fluid
i	inlet condition
m	mean condition
o	outlet condition

References

- [1] Tuckerman, D. B., "Heat-Transfer Microstructures for Integrated Circuits," *Ph.D. Thesis*, Department of Electronic Engineering, Stanford University, U.S.A. (1984).
- [2] Cross, W. T. and Ramshaw, C., "Process Intensification Laminar Flow Heat Transfer," *Chemical Engineering Research & Design: Transaction of the Institute of Chemical Engineers*, Vol. 64, pp. 258-294 (1986).
- [3] Friedrich, C. R. and Kang, S. W., "Micro Heat Exchangers Fabricated by Diamond Machining," *Precision Engineering*, Vol. 16, pp. 56-59 (1994).
- [4] Lee D. B., "Anisotropic Etching of Silicon," *Journal of Applied Physics*, Vol. 40, pp. 4569-4574 (1969).
- [5] Bean, K. E., "Anisotropic Etching of Silicon," *IEEE Trans. Electron Devices*, Vol. ED-25, pp. 1185 (1978).
- [6] Krause P. and Obermeyer E., "Etch and Surface Roughness of Deep Narrow U-Grooves in (110)-Orientated Silicon," *J. of Micromech. Microeng.*, Vol. 5, pp. 112-115 (1992).
- [7] Kays, W. M. and London A. L., "Compact Heat Exchangers," 3rd. ed. McGraw Hill Co. N.Y., U.S.A. (1964).
- [8] Arias, F., Oliver, S. R. J., Xu, B., Holmlin, R. E. and Whitesides, G. M., "Fabrication of Metallic Heat Exchangers Using Sacrificial Polymer Mandrils," *Journal of Microelectromechanical System*, Vol. 10, pp. 107-112 (2001).
- [9] Saji, N., Nagai, S., Tsuchiya, K., Asakura, H. and Obata, M., "Development of a compact

laminar flow heat exchanger with stainless steel micro-tubes,” *Physica C* 345, pp. 148-151 (2001).

***Manuscript Received: Mar. 21, 2002
and Accepted: Jun. 26, 2002***